

## Effects of nonlinearity on the time evolution of single-site localized states in periodic and aperiodic discrete systems

Magnus Johansson, Michael Hörnquist, and Rolf Riklund

*Department of Physics and Measurement Technology, Linköping University, S-581 83 Linköping, Sweden*

(Received 13 February 1995)

We perform numerical investigations of the dynamical localization properties of the discrete nonlinear Schrödinger equation with periodic and deterministic aperiodic on-site potentials. The time evolution of an initially single-site localized state is studied, and quantities describing different aspects of the localization are calculated. We find that for a large enough nonlinearity, the probability of finding the quasiparticle at the initial site will always be nonzero and the participation number finite for all systems under study (self-trapping). For the system with zero on-site potential, we find that the velocity of the created solitons will approach zero and their width diverge as the self-trapping transition point is approached from below. A similar transition, but for smaller nonlinearities, is found also for periodic on-site potentials and for the incommensurate Aubry-André potential in the regime of extended states. For potentials yielding a singular continuous energy spectrum in the linear limit, self-trapping seems to appear for arbitrarily small nonlinearities. We also find that the root-mean-square width of the wave packet will increase infinitely with time for those of the studied systems which have a continuous part in their linear energy spectra, even when self-trapping has occurred.

### I. INTRODUCTION

The study of the interplay between disorder and nonlinearity, providing two different mechanisms for localization, has received large attention in recent years.<sup>1,2</sup> As a simple model equation with applications in many different physical areas, the one-dimensional (1D) discrete nonlinear Schrödinger (DNLS) equation

$$i\frac{\partial\psi_n}{\partial t} = -\psi_{n+1} - \psi_{n-1} + a|\psi_n|^2\psi_n + V_n\psi_n \quad (1)$$

has been studied. This equation appears, for example, in the Holstein model for polaronic motion in solids,<sup>3</sup> in the Davydov model for transport of vibrational energy in proteins,<sup>4</sup> in models for the nonlinear optical response of superlattices,<sup>5</sup> and in models for nonlinear arrays of coupled waveguides.<sup>6</sup> The DNLS equation has two conserved quantities, the norm  $R = \sum_n |\psi_n|^2$  and the Hamiltonian

$$H = -\sum_n (\psi_n \psi_{n+1}^* + \psi_n^* \psi_{n+1}) + \frac{a}{2} \sum_n |\psi_n|^4 + \sum_n V_n |\psi_n|^2 \quad (2)$$

and is nonintegrable for systems with more than two sites. For disordered systems, i.e., when the on-site potential  $V_n$  is randomly chosen, the DNLS equation reduces with  $a=0$  to the 1D Anderson model,<sup>7</sup> for which the exponential localization of eigenstates has been rigorously proved.<sup>8</sup> In dynamical terms, this implies that an initially localized excitation will remain localized in a finite region and that the time-averaged probability to find the quasiparticle at the initially excited site will always be nonzero. When the on-site potential is randomly

distributed in the interval  $(-W, W)$  with  $W < 1$ , the dynamical localization has been shown<sup>9</sup> to be destroyed by the nonlinearity, in the sense that for  $|a| > a_c$  ( $a_c \sim 0.1$ ) the motion will be subdiffusive [i.e., the root-mean-square width  $\Delta n(t)$  of an initially localized wave packet will increase according to the law (7) below with  $\gamma = \frac{1}{5}$ ] for large times. Furthermore, for  $V_n \equiv 0$  the DNLS equation has been shown to exhibit self-trapping;<sup>10,11</sup> i.e., there exists a critical nonlinearity  $a_{st}$  such that for  $|a| > a_{st}$  the probability for an initially localized excitation to remain at the initial site will be significantly larger than 0. Using an energy balance condition, a value of  $a_{st} \approx 4$  for large chains was estimated in Ref. 11.

Recently, there has also been some interest<sup>12-17</sup> in the study of nonlinear models for systems which are aperiodically ordered, such as quasicrystals, incommensurate crystals, or aperiodic superlattices. In the linear regime, these systems exhibit a large variety of localization properties, depending on the specific nature of the aperiodicity. Many of these systems will already in the linear regime show anomalous diffuse behavior.<sup>18-22</sup> Thus it is interesting to compare the effect of adding nonlinearity to such a system with the corresponding effects in disordered and periodic systems discussed above. In this paper, we will study the dynamical localization properties for the DNLS equation when the wave packet is initially localized on one single site  $n_0$ . We may without loss of generality write

$$\psi_n(0) = \delta_{n, n_0}, \quad (3)$$

since the non-normalized case  $R \neq 1$  can be mapped to the case  $R = 1$  by the rescaling  $\psi_n \rightarrow \psi_n / \sqrt{R}$ ,  $a \rightarrow aR$ . We will compare the results obtained for some specific choices of the deterministic aperiodic on-site potential,

having qualitatively different localization properties in the linear limit. As measures of the localization, we will use the probability of finding the excitation at the initial state

$$W_0(t) = |\psi_{n_0}(t)|^2, \quad (4)$$

the mean-square displacement

$$[\Delta n(t)]^2 = \sum_n (n - n_0)^2 |\psi_n(t)|^2, \quad (5)$$

and the participation number

$$P(t) = \left\{ \sum_n |\psi_n(t)|^4 \right\}^{-1}. \quad (6)$$

The time evolution of the root-mean-square displacement  $\Delta n$  will normally follow a power law

$$\Delta n(t) \sim t^\gamma, \quad (7)$$

indicating whether the motion is localized ( $\gamma=0$ ), subdiffusive ( $0 < \gamma < \frac{1}{2}$ ), diffusive ( $\gamma = \frac{1}{2}$ ), superdiffusive ( $\frac{1}{2} < \gamma < 1$ ), ballistic ( $\gamma=1$ ), or superballistic ( $\gamma > 1$ ), while the participation number gives a rough estimation of the number of sites where the wave packet has a significant amplitude ( $P=1$  for a single-site localized state and  $P=N$  for a state uniformly extended over  $N$  sites). We will begin by analyzing the cases  $V_n \equiv 0$  and  $V_n$  periodic in Sec. II, where it is emphasized how the above-defined quantities (4)–(6) measure different aspects of the dynamical localization. In particular, the signatures of a self-trapping transition are discussed. In Sec. III we discuss incommensurate models, where the on-site potential takes a continuous set of values, and in Sec. IV some examples of binary substitutionally generable systems are studied.

The DNLS equation (1) is integrated numerically,

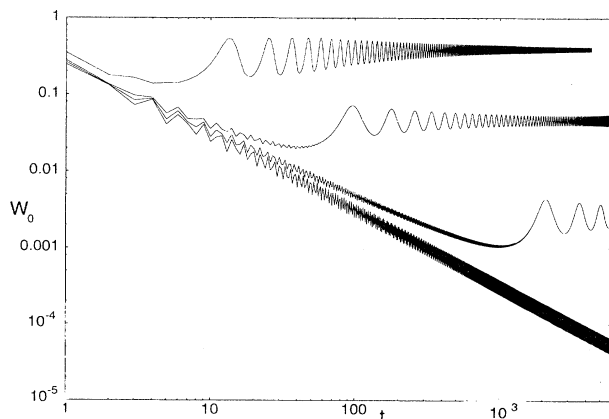


FIG. 1. Initial-site probability  $W_0$  as a function of time  $t$  for model (1) with  $V_n \equiv 0$  and, from bottom to top in the figure,  $a = -3.4, -3.5, -3.6,$  and  $-4.0$ , respectively. For  $|a| < 3.4$ ,  $W_0$  will decrease following the same slope as for  $|a| = 3.4$ , but with larger fluctuations. For  $|a| > 4.0$ , the time average of  $W_0$  will continue to increase toward 1.

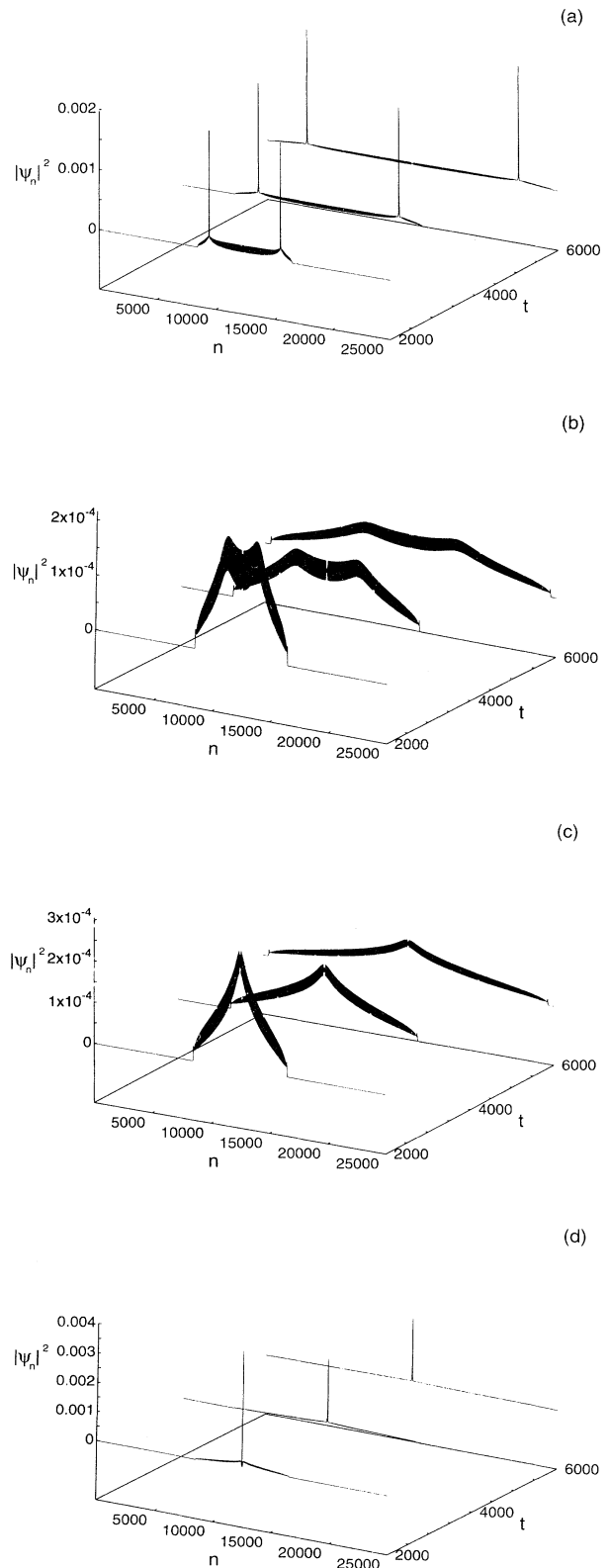


FIG. 2. Probability distribution  $|\psi_n|^2$  of the wave functions at times  $t=2000, 4000,$  and  $6000$  when  $V_n \equiv 0$  and (a)  $a = -2.80$ , (b)  $a = -3.40$ , (c)  $a = -3.48$ , and (d)  $a = -3.50$ . The initial site is  $n_0 = 12500$  in all cases.

mainly by using a variable-step variable-order Adams method from the NAG library. In order to eliminate the influence of numerical errors, the calculations reported here have been checked by comparing with results obtained using different algorithms (e.g., Runge-Kutta methods of different order and other implementations of Adams methods), different error tolerances, and different precisions. For the periodic systems and also for small nonlinearities in the aperiodic systems, we find that the integration can easily be performed for long times with very small errors in the results, while for some of the aperiodic systems with larger nonlinearities numerical errors become appreciable already after a few thousand time steps. In any case, the results presented here have been checked to be correct to at least three significant digits for all times. Since our purpose is to simulate infinite chains, we exclude the influence of the boundary conditions by studying systems large enough so that the wave packet will have a negligible amplitude at the end points during the integration time (in most cases  $|\psi_n|^2 < 10^{-30}$  near the boundaries).

## II. PERIODIC CASE

For  $V_n \equiv 0$ , the self-trapping transition was estimated in Ref. 11 to occur when the energy of the initial single-site state, obtained from (2), falls outside the energy band corresponding to delocalized, equipartitioned states, which gives the value  $|a_{st}| = 4$  for an infinite chain. However, it was noted that this condition only gives a rough location of the self-trapping transition and that some self-trapping occurs already below this value. We will show below, mainly by direct inspection of the time-evolved wave function, that the actual transition occurs for a somewhat smaller nonlinearity ( $|a_{st}| \approx 3.45$ ). We will also see that when a periodic on-site potential is added the transition occurs even earlier and that in this case the energy-balance condition does not give even a rough estimate of the location of the transition.

Of our three measures (4)–(6), the initial-site probability  $W_0$  is the most natural to use when studying the self-

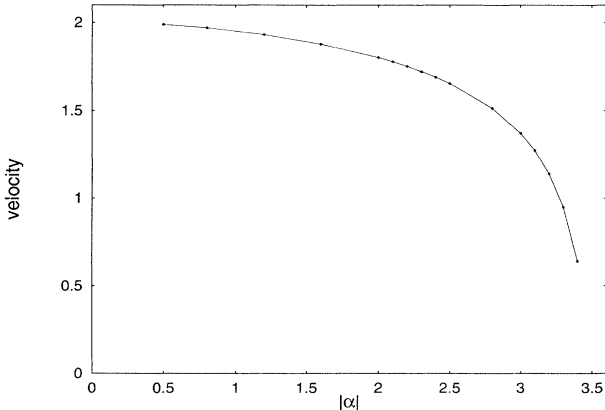


FIG. 3. Soliton velocity as a function of nonlinearity  $a$  in the non-self-trapping region when  $V_n \equiv 0$ . The solid line is a guide to the eye.

trapping transition. In Fig. 1 we show how the initial-site probability varies with time for some different values of  $a$  when  $V_n \equiv 0$  ( $a$  is chosen to be negative in the figure, but when  $V_n \equiv 0$  the behavior will be the same for positive  $a$ ). From this figure, it is obvious that there will always be a finite probability to find the quasiparticle at the initial site when  $|a| \gtrsim 3.5$ , but for smaller  $|a|$  this probability seems to decay to 0 as  $t \rightarrow \infty$ . To get a physical picture of what causes this transition, we show in Fig. 2 the time evolution of the wave packet for some values of  $a$  around the transition point. As can be seen, for  $|a| \lesssim 3.4$  the wave packet will develop partly into two solitonlike objects moving in opposite directions away from the start site and partly into an oscillating state having an approximately constant, time-decaying amplitude. As  $|a|$  increases from zero, the width of the solitons will first decrease until  $|a| \approx 2.1$  and then increase until  $|a|$  reaches the point of the self-trapping transition, where the soliton widths seem to diverge. Also, the velocity of the solitons will decrease monotonically as  $|a|$  is increased from zero, as can be seen from Fig. 3. The soliton velocity will be close to the velocity of the wave front of the oscillating state when  $|a|$  is small and apparently approaches zero as

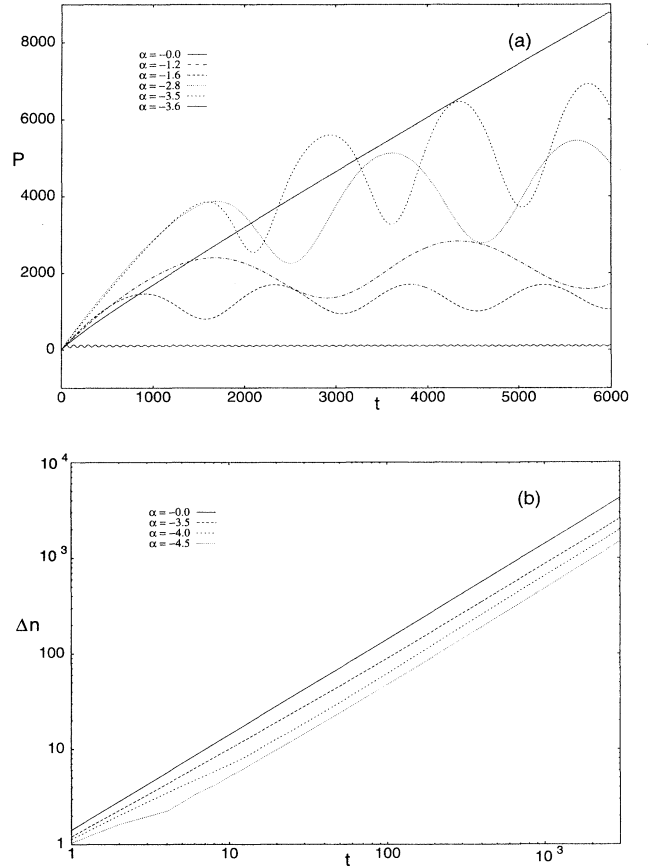


FIG. 4. Time evolution of (a) the participation number  $P(t)$  and (b) the root-mean-square width  $\Delta n(t)$  for different nonlinearities when  $V_n \equiv 0$ . In (a), we have  $a = 0, -3.5, -2.8, -1.2, -1.6,$  and  $-3.6$  from top to bottom at  $t = 6000$  and in (b)  $a = 0, -3.5, -4.0,$  and  $-4.5$  from top to bottom.

$|a| \rightarrow |a_{st}|$ . Increasing  $|a|$  beyond the transition point will result in one single solitonlike object localized around the start site. The width of this single, self-trapped, soliton decreases fast for increasing  $|a|$ , resulting in a large amplitude on the start site.

To see how the other quantities are affected by the self-trapping transition, we plot in Figs. 4(a) and 4(b) the participation number and the root-mean-square displacement, respectively, as a function of time for different  $a$ . We see that the participation number increases linearly with time for all times when  $a=0$ , indicating a uniform spreading over the chain. When  $|a|$  is increased from zero,  $P$  will for an initial time period increase linearly with time, the slope of the line increasing for increasing  $|a|$ , but finally the curve will bend over and the participation number will begin to oscillate. We attribute these oscillations to the formation and subsequent “breathing” of the two solitonlike objects discussed above, the maxima (minima) in  $P$  corresponding to maximal (minimal) width and minimal (maximal) amplitude of the solitons. As  $|a|$  is increased further,  $P$  will initially oscillate faster and with a smaller mean value until  $|a| \approx 2.1$ , indicating a decreasing soliton width, but as  $|a|$  approaches  $|a_{st}| \approx 3.45$  the oscillations will be slower and the maximum value of  $P$  will increase as a result of the broadening of the solitons. It is possible that the maximum value of  $P$  may be infinite just at the transition point, but of course our numerical calculations cannot guarantee this. Increasing  $|a|$  beyond the transition point will rapidly decrease both the period of the oscillations and the maximum value of  $P$ , since the width of the single soliton rapidly decreases when entering the self-trapping region.

From Fig. 4(b) we find the perhaps somewhat surprising result that the root-mean-square deviation will follow the ballistic law (7) with  $\gamma=1$  independent of the nonlinearity for large times. For  $|a| > |a_{st}|$ , however, we note on closer look that the time evolution of  $\Delta n$  can be roughly divided into four different regions. After an initial period of ballistic motion, the curve bends over showing a smaller slope for  $t_1 < t < t_2$ , which is the time period where the formation of the self-trapped soliton occurs. Following this, we observe a time interval  $t_2 < t < t_3$  where the slope of the curve grows to a value which is actually larger than 1, indicating some kind of superballistic motion. Finally, for  $t > t_3$  the normal ballistic motion is retained. As the nonlinearity is increased  $t_1$ ,  $t_2$ , and  $t_3$  will all decrease, and for large nonlinearities the final, ballistic region will be observed almost immediately. The fact that the motion is ballistic also for  $|a| > |a_{st}|$  can be understood by realizing that there will always be some amount of probability amplitude “escaping” from the initial site before the self-trapped state is formed. This escaping probability will be small if  $|a|$  is large, and thus, because of the smallness of the term  $a|\psi_n|^2$  in (1), the time evolution of this part of the wave will only be weakly affected by the nonlinearity. We also note that although  $\Delta n$  grows linearly with time for all  $|a|$  when  $t$  is large, its value at a specific time will decrease as  $|a|$  is increased in the self-trapping region as a result of the decreasing amount of escaping probability.

To study the effect of introducing a simple periodic

on-site potential  $V_n$  in the DNLS equation (1), we now discuss the results obtained when the potential is chosen as

$$V_n = V_0(-1)^n. \quad (8)$$

In Figs. 5(a) and 5(b) we show the variation of the initial-site probability with time for different nonlinearities ( $a < 0$ ) when  $V_0=1$  and the start site  $n_0$  is odd and even, respectively. As can be seen, we also here get a self-trapping transition, but for smaller values of  $|a|$ ,  $|a_{st,odd}| \approx 1.55$  and  $|a_{st,even}| \approx 1.70$ , respectively. (When  $a$  is positive, these values will be interchanged, since it is the relative sign between  $a$  and  $V_{n_0}$  that is of importance.)

We also find that the values of  $|a_{st}|$  decrease as the amplitude  $V_0$  is increased (see Fig. 6). The basic mechanism behind the transition appears to be the same as for  $V_n \equiv 0$ , and the participation number and root-mean-square deviation behave in a qualitatively similar manner as described above. Also, here, the motion will be ballistic for large times, independent of the nonlinearity. As we remarked in the beginning of this section, we cannot

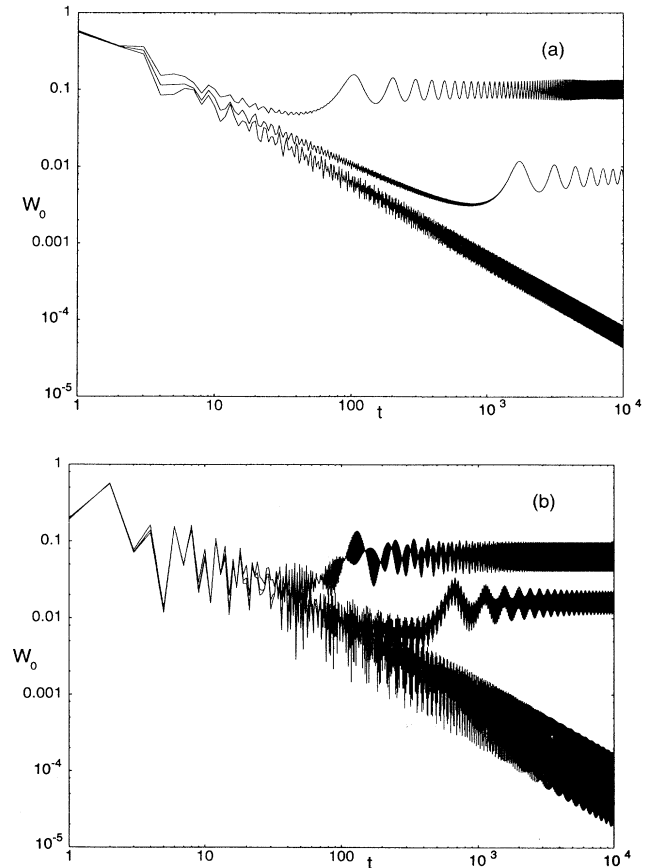


FIG. 5. Initial-site probability  $W_0$  vs time  $t$  for model (1) with the periodic on-site potential (8) when (a)  $V_{n_0} = -1$  (odd start site) and (b)  $V_{n_0} = +1$  (even start site) and different nonlinearities. From bottom to top in the figures, we have in (a)  $a = -1.50, -1.60$ , and  $-1.70$  and in (b)  $a = -1.70, -1.75$ , and  $-1.85$ .

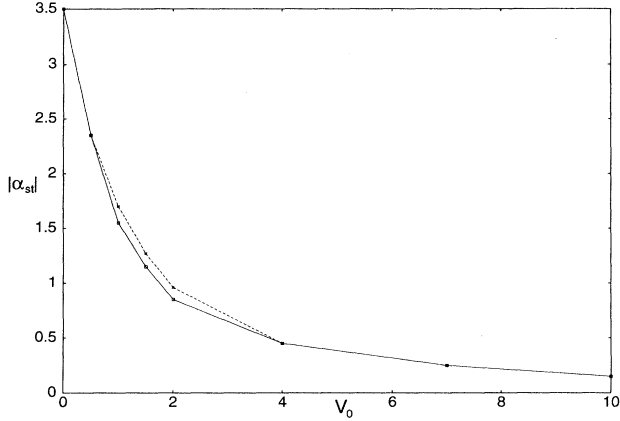


FIG. 6. Location of the self-trapping transition  $|\alpha_{st}|$  as a function of potential amplitude  $V_0$  for the periodic on-site potential (8). The upper (dashed) curve corresponds to the case when the nonlinearity  $a$  has opposite sign to the potential amplitude  $V_{n_0}$  at the initial site, while the lower (solid) curve corresponds to equal signs.

use the simple energy-balance condition from Ref. 11 to get even a rough estimation of the location of the transition point in this case. For example, since the initial single-site energy is given by  $H_{SS} = a/2 + V_{n_0}$ , this condition used in its original form estimates the difference  $|a_{st,even} - a_{st,odd}|$  to be of the order of 4 when  $V_0=1$ , which is a large overestimation of the difference ( $\sim 0.15$ ) we obtained numerically. It may be possible to formulate modified conditions of this kind by considering the band structure of the energy spectrum for the linear models, but we will not exploit this possibility further here.

### III. INCOMMENSURATE MODELS

The perhaps most well-known and studied model for one-dimensional incommensurate crystals is the Aubry-André model,<sup>23</sup> which is the nearest-neighbor tight-binding model [Eq. (1) with  $a=0$  and  $\psi_n(t) = c_n e^{-iEt}$ ] obtained by choosing the on-site potential as

$$V_n = V_0 \cos(2\pi n \xi), \quad (9)$$

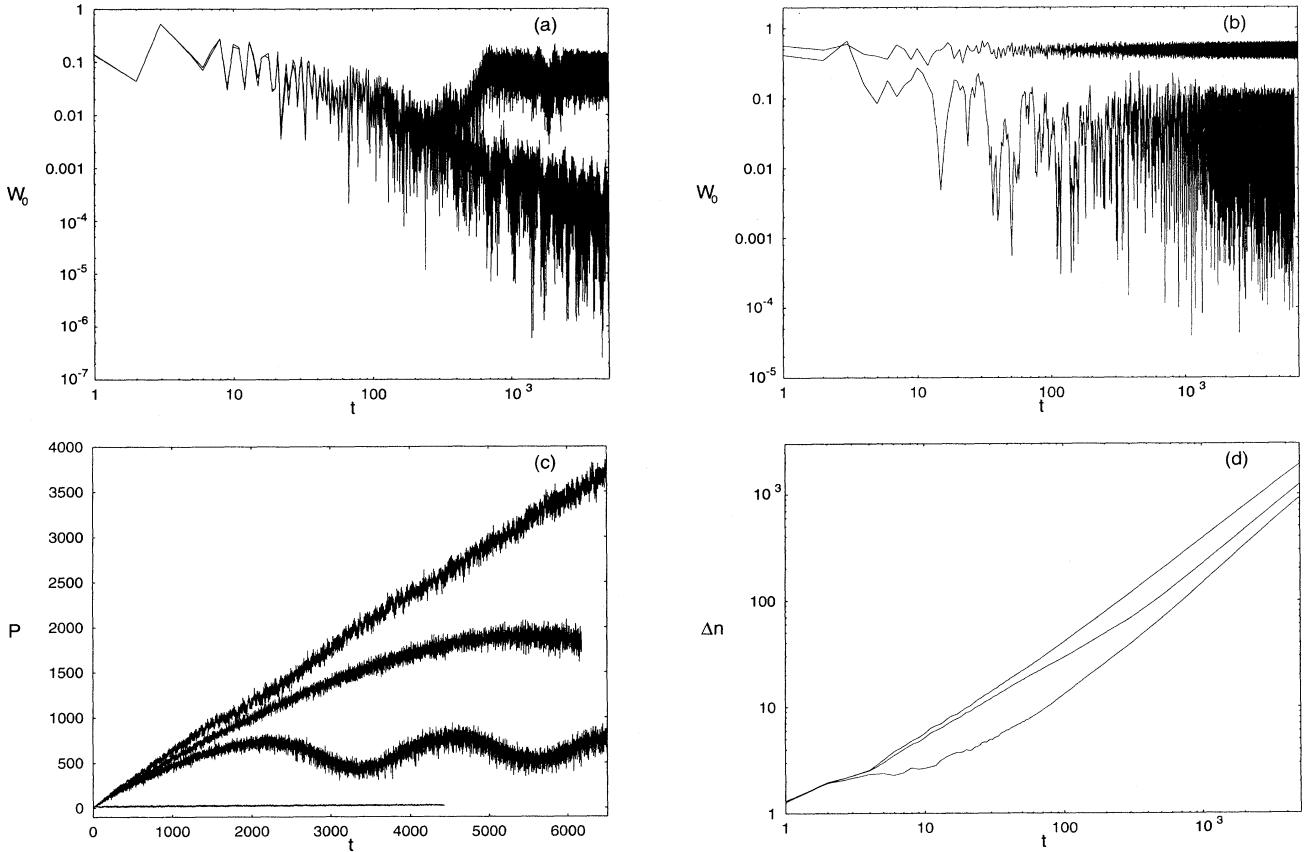


FIG. 7. Time evolution of (a), (b) the initial-site probability  $W_0(t)$ , (c) the participation number  $P(t)$ , and (d) the root-mean-square width  $\Delta n(t)$  for the DNLS equation (1) with the incommensurate Aubry-André potential (9) with  $V_0=1.5$  and different nonlinearities  $a$  and initial sites  $n_0$ . In (a) we have  $n_0=5000$  ( $V_{n_0} \approx 1.5 \times 0.48$ ) and  $a=-0.7$  (lower curve) and  $a=-0.8$  (upper curve); in (b),  $n_0=0$  ( $V_{n_0}=1.5$ ) and  $a=-0.6$  (lower curve) and  $a=+0.6$  (upper curve); in (c),  $n_0=6000$  ( $V_{n_0} \approx 1.5 \times 0.29$ ) and  $a=0, -0.6, -0.7$ , and  $-1.0$ , respectively, from top to bottom in the figure; and in (d),  $n_0=5000$  and  $a=0, -0.8$ , and  $-2.0$  from top to bottom.

with  $\zeta$  irrational. For this model, the spectrum of allowed energies  $E$  for an infinite chain is absolutely continuous with all states extended if  $V_0 < 2$ , singular continuous with all states critical if  $V_0 = 2$ , and pure point with all states localized if  $V_0 > 2$  for almost all  $\zeta$ . Dynamically, the evolution of an initially localized state is found<sup>18,19</sup> to be ballistic if  $V_0 < 2$ , close to diffusive ( $\gamma \approx 0.5$ ) if  $V_0 = 2$ , and localized if  $V_0 > 2$ . These results are consistent with the conjecture<sup>19</sup> that the exponent  $\gamma$  in (7) should be equal to the Hausdorff dimension of the energy spectrum and the rigorous result<sup>24</sup> that diffusive spread over one-dimensional lattices can take place only if the spectrum is singular continuous. We will in this section study the nonlinear model (1) with the Aubry-André potential (9). (A similar, but more complex, model was studied in Ref. 14 where the dynamics of polarons in a coupled electron-lattice system with the electron-lattice interaction taken as a symmetrized deformation potential was investigated.) In our numerical computations, we choose the incommensurability to be equal to the golden mean, i.e.,  $\zeta = (\sqrt{5} + 1)/2$ , but we believe that the qualitative behavior should be the same for almost all  $\zeta$ , as is the case for the linear model. At the end of this section, we will also discuss a related model whose linear spectrum possesses a mobility edge.

For subcritical values of the modulation amplitude ( $V_0 < 2$ ) in (9), we find a self-trapping transition in a similar way as described in Sec. II. As an example, we show in Fig. 7(a) the initial-site probability  $W_0(t)$  for the case with  $V_0 = 1.5$ ,  $n_0 = 5000$  (giving  $V_{n_0} \approx 1.5 \times 0.48$ ),  $a = -0.7$ , and  $-0.8$ . Apparently, the self-trapping transition occurs somewhere between these values. The exact location of the transition point depends on the value of the potential on the start site, resulting here in a variation for  $|a_{st}|$  between approximately 0.3 and 0.9, where the smaller value is obtained when  $|V_{n_0}|$  is close to 1.5 and the larger value when  $|V_{n_0}|$  is close to 0. However, the transition occurs earlier for the incommensurate potential than for the periodic potential (8), where  $|a_{st}| \approx 1.1 - 1.3$  when  $V_0 = 1.5$  (see Fig. 6). It is also interesting to note that although the value of  $|a_{st}|$  for the incommensurate model is only weakly dependent on the relative sign between  $a$  and  $V_{n_0}$ , the self-trapping for  $|a| > |a_{st}|$  will be much more efficient when these quantities have the same sign. This can be seen from Fig. 7(b), where the initial-site probability is shown for  $n_0 = 0$  ( $V_{n_0} = +1.5$ ) and  $a = -0.6$  and  $+0.6$ . (For this case,  $a_{st} \approx -0.4$  and  $+0.3$ .) By studying the participation number for this case (not shown in the figure), we find that when  $a = +0.6$  (equal signs) the main part of the wave packet will be spread only over approximately five sites, while it will be spread over as much as approximately 100 sites when  $a = -0.6$  (different signs). Generally, the qualitative behavior of  $P(t)$  and  $\Delta n(t)$  in the subcritical regime  $V_0 < 2$  is similar as for the periodic cases, as shown in Figs. 7(c) and 7(d), respectively. However, from Fig. 7(d) we note that for  $|a| > |a_{st}|$  there is a more pronounced difference between the four different time regimes in the evolution of  $\Delta n$  than for  $V_n \equiv 0$ , so

that, for example, the exponent  $\gamma$  in (7) takes for  $a = -3$  (not shown in the figure) a value as large as 1.36 in the superballistic region  $100 \lesssim t \lesssim 1000$ . We also note that although  $\gamma$  may be substantially larger than 1 for large times, it always seems to approach 1 as  $t \rightarrow \infty$ .

When increasing the modulation amplitude  $V_0$ ,  $|a_{st}|$  will decrease, and as  $V_0$  approaches the critical value  $V_0 = 2$ , we find that an arbitrarily small nonlinearity appears to be enough to cause self-trapping. However, although the time-averaged initial-site probability always seems to be nonzero and the participation number saturates at finite values for  $V_0 = 2$  and arbitrary  $a$ , the root-mean-square width will also here continue to increase for all times. This can be seen from Fig. 8, where  $\Delta n(t)$  is shown for different values of  $a$  when  $V_0 = 2$ . After the initial time interval of diffusive or almost diffusive motion (the length of this interval decreases for increasing nonlinearity), the motion will in the general case be subdiffusive, with typical exponents  $\gamma$  varying between approximately 0.25 and 0.4. This is in contrast to the behavior reported for the model in Ref. 14, where also  $\Delta n$  was found to saturate.

When  $V_0 > 2$ , the wave packet will remain localized for all times in the linear model. Its width will only increase during an initial, transient time period, and there will be an upper limit value of  $\Delta n$ . For the nonlinear model, one might expect a similar behavior as obtained for the disordered model in Ref. 9, i.e., that there will be a subdiffusive spread for large times. Our numerical calculations show that also here there is a qualitative difference between the cases when the nonlinearity and potential amplitude at the start site have equal or different signs. We show, in Figs. 9(a) and 9(b),  $\Delta n(t)$  for some different (negative) values of  $a$  when  $n_0 = 250$  [ $V_{n_0} \approx 2.7 \times (-0.999)$ ] and  $n_0 = 0$  ( $V_{n_0} = +2.7$ ), respectively. From Fig. 9(a) we see that when the signs are equal the nonlinearity will increase the localization, while in Fig. 9(b) it is shown that the nonlinearity may cause

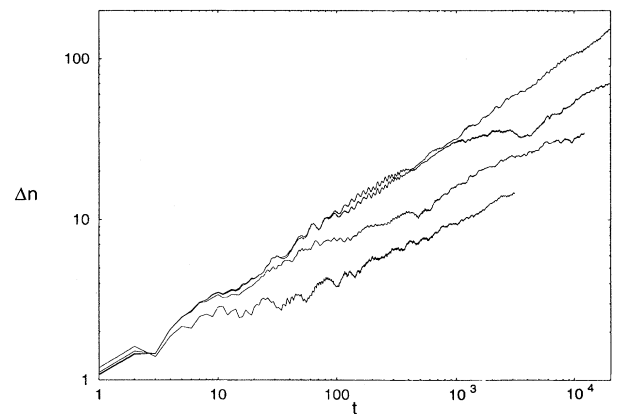


FIG. 8. Root-mean-square width  $\Delta n$  vs time  $t$  for the DNLS equation (1) with the Aubry-André on-site potential (9) with  $V_0 = 2$ ,  $n_0 = 3000$  ( $V_{n_0} \approx 2 \times 0.80$ ), and  $a = 0, -0.1, -0.4$ , and  $-1.5$  from top to bottom in the right half of the figure.

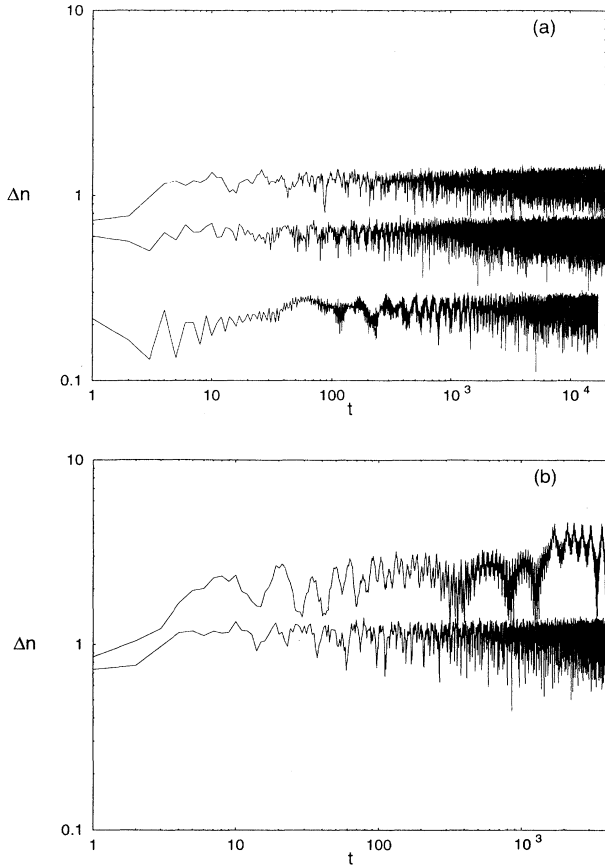


FIG. 9. Root-mean-square width  $\Delta n$  as a function of time  $t$  for Eq. (1) with the Aubry-André on-site potential (9) with  $V_0 = 2.7$  and different nonlinearities  $a$  and initial sites  $n_0$ . In (a) we have  $n_0 = 250$  ( $V_{n_0} \approx -2.7 \times 0.9986$ ) and  $a = 0$  (upper curve),  $a = -1$  (middle curve), and  $a = -10$  (lower curve); and in (b),  $n_0 = 0$  ( $V_{n_0} = 2.7$ ) and  $a = 0$  (lower curve), and  $a = -1$  (upper curve).

the wave packet to be less localized when the signs are unequal ( $a = -1.0$  in the figure). However, we cannot tell whether  $\Delta n$  will continue to increase subdiffusively, since in this case (when the wave packet is very localized and the nonlinearity is rather large) we are unable to obtain accurate results from the numerical integration procedure for more than a few thousand time steps using a reasonable amount of computer time. We have also found that for even larger nonlinearities (e.g.,  $a = -10$ ) the localization will increase (at least in the time region where our numerical results are accurate) also for the case with unequal signs.

As a model for incommensurate systems, the Aubry-André model is exceptional because of the energy-independent metal-insulator transition at  $V_0 = 2$  and the existence of a purely singular continuous spectrum. Generically, models with continuous on-site potential have for intermediate modulation amplitudes an energy spectrum consisting of regions of absolutely continuous and point spectrum separated by one or several mobility

edges.<sup>25</sup> We have studied the model obtained by taking the negative of the absolute value of the Aubry-André potential, i.e.,

$$V_n = -V_0 |\cos(2\pi n \xi)|. \quad (10)$$

The linear version of this model has for small  $V_0$  only extended states and for large  $V_0$  only localized states just as the Aubry-André model, but for  $2 \lesssim V_0 \lesssim 7$  the spectrum contains one mobility edge separating extended states with low energy from localized states with high energy.<sup>26</sup> Dynamically, this linear model will also behave similar as the Aubry-André model for small or large potential amplitudes. For intermediate values of  $V_0$ , the existence of localized states will cause the initial-state probability to be nonzero and the participation number to be finite, while the extended states will contribute to a ballistic spread of the width of the wave packet as  $t \rightarrow \infty$ . Introducing nonlinearity will in general for these values increase the localization properties as described by the participation number and initial-site probability, while the ballistic spread is retained for large  $t$ . An example of this is shown in Fig. 10. Note that for this model  $V_{n_0}$  is al-

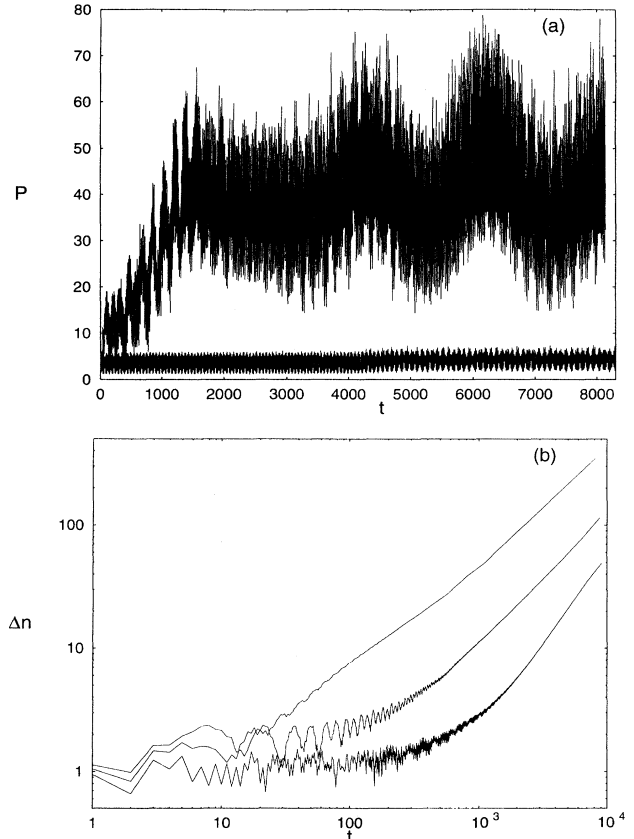


FIG. 10. (a) Participation number  $P$  and (b) root-mean-square width  $\Delta n$  as a function of time  $t$  for the incommensurate model with on-site potential given by (10) with  $V_0 = 6$ . In (a) we have  $a = 0$  (upper curve) and  $a = +1$  (lower curve), while, in (b),  $a = 0, +1,$  and  $-1$  from top to bottom in the right half of the figure. (For  $t \lesssim 10$ ,  $a = +1$  yields larger values of  $\Delta n$  than  $a = 0$ .) The initial site is  $n_0 = 0$  ( $V_{n_0} = -6$ ) in all cases.

ways negative and that a negative  $a$  will cause the wave packet to be more localized than a positive  $a$ , in agreement with the results obtained above.

#### IV. BINARY APERIODIC SYSTEMS

In describing properties of one-dimensional quasicrystals and aperiodic superlattices, one often studies tight-binding models of the type (1) with on-site potentials taking a finite number of values. One standard way of generating such potentials is by using a substitution rule to generate an infinite binary sequence of letters. For instance, the Fibonacci sequence is generated by the rule

$$A \rightarrow AB, \quad B \rightarrow A, \quad (11)$$

acting on a seed  $A$ ; i.e., the first generations of the sequence are given by  $A, AB, AB A, AB A AB, AB A AB A, \dots$ . The on-site potential is then obtained by choosing  $V_n = +V_0$  if site  $n$  is an  $A$  and  $V_n = -V_0$  if site  $n$  is a  $B$ . For the linear model [ $a=0$  in (1)], the Fibonacci system,<sup>27</sup> as well as a large class of substitutionally generated aperiodic systems,<sup>28</sup> has been shown to exhibit a purely singular continuous energy spectrum. Dynamically, this type of spectrum generally leads to anomalous diffusive spread of an initially localized wave function, the index  $\gamma$  in (7) continuously decreasing from 1 to 0 as the site amplitude  $V_0$  increases from 0 to infinity.<sup>19,20</sup> We will in this section study the effect of adding nonlinearity to such systems. We will also discuss the Rudin-Shapiro sequence, for which the general sufficient conditions for singular continuous energy spectrum obtained in Ref. 28 are not applicable.

For the binary systems which in the linear limit exhibit singular continuous energy spectrum, we find that introduction of the nonlinear term in (1) has a similar effect as for the Aubry-André model with  $V_0=2$ . As examples, we show, in Fig. 11,  $\Delta n(t)$  for (a) the Fibonacci model, (b) the Thue-Morse model, and (c) the period-doubling model. The Thue-Morse sequence is generated by the substitution rule

$$A \rightarrow AB, \quad B \rightarrow BA \quad (12)$$

and the period-doubling sequence by the rule

$$A \rightarrow AB, \quad B \rightarrow AA. \quad (13)$$

Both these sequences have been rigorously proved to give a singular continuous spectrum for the linear model.<sup>29</sup> As can be seen from Fig. 11, the root-mean-square width of the wave packet will in general show different behavior for different time regimes, and at least for the Thue-Morse and period-doubling systems rather large regimes of superballistic transport can be noted. From Fig. 11(a) we also note that the index  $\gamma$  decreases with increasing nonlinearity for large  $t$  for the Fibonacci system, as for the Aubry-André model with  $V_0=2$ , while no such tendency can be noted for the Thue-Morse or period-doubling systems in the time regime shown in Fig. 11. However, none of the systems show any signs of saturation of  $\Delta n$  for large  $t$ .

The binary Rudin-Shapiro sequence can be generated

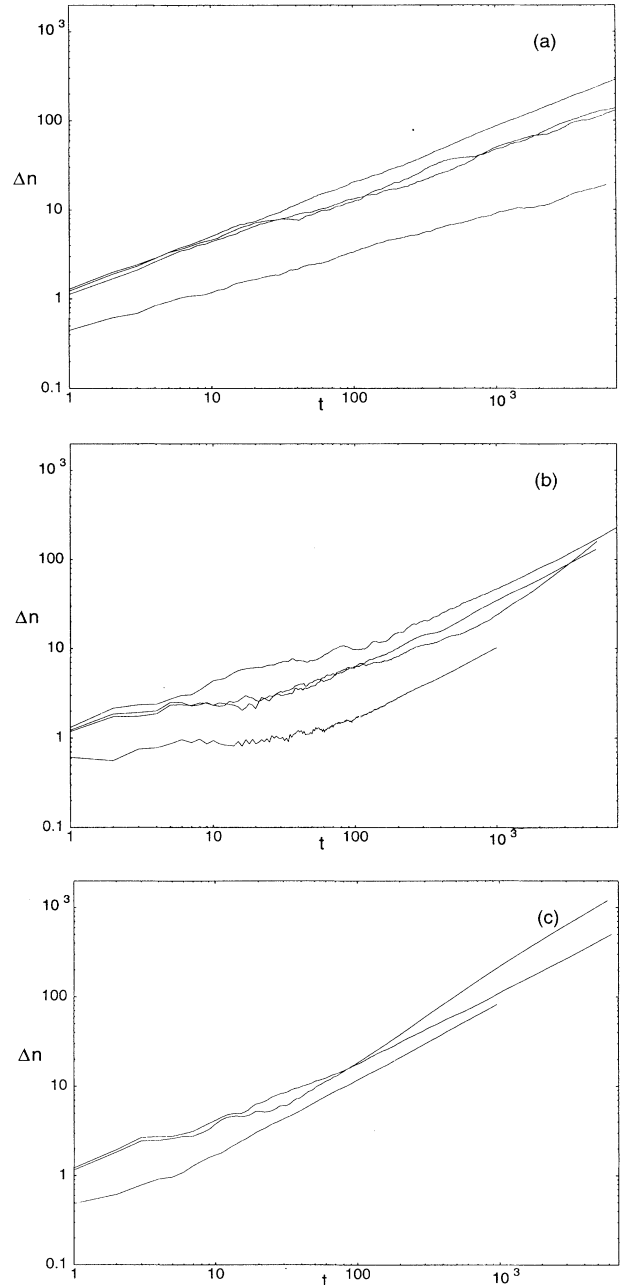


FIG. 11. Root-mean-square width  $\Delta n$  as a function of time  $t$  for different nonlinearities when the on-site potential  $V_n$  is obtained from (a) the Fibonacci sequence, (b) the Thue-Morse sequence, and (c) the period-doubling sequence. In (a) we have  $a=0, -1.0, +1.0,$  and  $-5.0$  from top to bottom at  $t=5000$ ; in (b),  $a=0, -1.2, -1.6,$  and  $-5.0$  from top to bottom at  $t=1000$ ; and in (c),  $a=-0.8, 0,$  and  $-5.0$  from top to bottom at  $t=1000$ . The initial site is  $n_0=3000$  in (a) and  $n_0=8192$  in (b) and (c) ( $V_0=1.0$  and  $V_{n_0}=-1.0$  in all cases).

by the four-letter substitution rule

$$A \rightarrow AB, \quad B \rightarrow AC, \quad C \rightarrow DB, \quad D \rightarrow DC, \quad (14)$$

where in the final chain each  $A$  and  $B$  are associated with

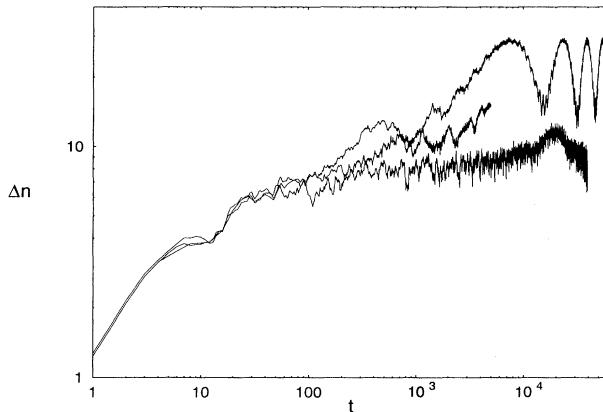


FIG. 12. Root-mean-square width  $\Delta n$  as a function of time  $t$  for Eq. (1) with the Rudin-Shapiro on-site potential obtained from (14) with  $V_0=1.0$  and initial site  $n_0=1024$  ( $V_{n_0}=-1.0$ ). In the figure,  $a=0$  (upper curve for  $t>1000$ ),  $a=+0.1$  (lower curve), and  $a=+0.5$  (middle curve). Note that for  $a=0.5$  the wave packet will be less localized than for  $a=0.1$ , but still more localized than for the linear case in the time regime where the integration procedure is accurate.

an on-site potential  $V_n = +V_0$  and each  $C$  and  $D$  are associated with  $V_n = -V_0$ . The Rudin-Shapiro sequence is exceptional among the binary substitutionally generable systems in many ways; e.g., the Fourier intensity measure of the sequence is absolutely continuous as for a random sequence,<sup>30</sup> and numerical investigations<sup>21,31</sup> of the linear tight-binding equation have indicated a pure point energy spectrum with normalizable but mainly weaker than exponentially localized eigenstates for almost all values of  $V_0$ . Dynamically, the exponent  $\gamma$  in (7) was found to be zero for large  $t$  except when the potential amplitude  $V_0$  takes one of the exceptional values for which non-normalizable eigenstates exist. In the latter case, a subdiffusive behavior was found.<sup>21</sup> When introducing nonlinearity, we find that the localization will normally be increased, at least for the time region where our numerical integration procedure yields reliable results. An example of this is shown in Fig. 12, showing  $\Delta n(t)$  when  $a=0$ ,  $a=+0.1$ , and  $a=+0.5$  for the case  $V_0=1$ , where all states are normalizable for the linear model. As for the Aubry-André model in the localized regime, we find that when  $|a| \gtrsim 0.5$  the growing of numerical errors will in practice prevent us from performing the integration for more than a few thousand time steps, and so the possibility of a subdiffusive behavior as  $t \rightarrow \infty$ , as obtained for the disordered model, cannot be excluded in this case either.

## V. SUMMARY

The localization properties of the one-dimensional discrete nonlinear Schrödinger equation (1) have been in-

vestigated by studying the effect of varying the nonlinearity parameter  $a$  on the time evolution of an initially single-site localized state for different periodic and deterministic aperiodic on-site potentials  $V_n$ . In general, we find that self-trapping will always occur if  $|a|$  is large enough and that the self-trapping will be more efficient when  $a$  has the same sign as the potential amplitude on the initial site. When  $V_n \equiv 0$ , the transition is found to occur at  $|a_{st}| \approx 3.45$ , corresponding to a point of zero velocity and diverging width for the two solitons created for  $|a| < |a_{st}|$ . For periodic on-site potentials,  $|a_{st}|$  decreases as the amplitude  $V_0$  increases, being, however, nonzero also for large values of  $V_0$ . A similar behavior is found for the incommensurate Aubry-André model in the subcritical regime  $V_0 < 2$ , but for this model  $|a_{st}| \rightarrow 0$  as  $V_0 \rightarrow 2$ , where the energy spectrum of the linear model becomes singular continuous. Also for other models exhibiting a singular continuous energy spectrum in the linear limit, such as the Fibonacci, Thue-Morse, and period-doubling models, self-trapping apparently occurs for an arbitrarily small nonlinearity. For all these systems, we find that the root-mean-square width of the wave packet will continue to increase for all times also when self-trapping has occurred, indicating ballistic motion if the corresponding linear energy spectrum has an absolutely continuous part and anomalous diffusion for systems whose linear counterparts exhibit a purely singular continuous spectrum. When the eigenstates of the linear model are localized, as for the golden-mean Aubry-André model with  $V_0 > 2$  and the Rudin-Shapiro model for almost all  $V_0$ , we have found cases where the localization has been weakened by the introduction of nonlinearity. However, because of the rapid growth of numerical errors in the integration procedure for these cases, we have not been able to study a sufficiently long time interval to say whether there will be a subdiffusive spread of the wave packet when  $t \rightarrow \infty$ , as found in Ref. 9 for a random on-site potential, or whether the wave packet will remain localized for all times also in the presence of nonlinearity. As a final remark, we stress that even in the presence of nonlinearity the properties of the energy spectrum of the linear model are most important to the dynamical localization properties and that the different aperiodic models in this sense provide a wide class of systems with qualitatively different properties also for the nonlinear case.

## ACKNOWLEDGMENTS

Financial support from the Swedish Natural Science Research Council is gratefully acknowledged. Access to the computer facilities at the National Supercomputer Center in Sweden at Linköping University has been very valuable in performing the numerical calculations in this work.

- <sup>1</sup>S. A. Gredeskul and Yu. S. Kivshar, *Phys. Rep.* **216**, 1 (1992), and references therein.
- <sup>2</sup>*Disorder and Nonlinearity*, edited by A. R. Bishop, D. K. Campbell, and S. Pnevmatikos, Springer Proceedings in Physics Vol. 39 (Springer-Verlag, Berlin, 1989); *Nonlinearity with Disorder*, edited by F. Abdullaev, A. R. Bishop, and S. Pnevmatikos, Springer Proceedings in Physics Vol. 67 (Springer-Verlag, Berlin, 1992).
- <sup>3</sup>T. Holstein, *Ann. Phys. (N.Y.)* **8**, 325 (1959); L. A. Turkevich and T. D. Holstein, *Phys. Rev. B* **35**, 7474 (1987).
- <sup>4</sup>A. S. Davydov, *Solitons in Molecular Systems* (Reidel, Dordrecht, 1985); *Davydov's Soliton Revisited*, edited by P. L. Christiansen and A. C. Scott (Plenum, New York, 1990).
- <sup>5</sup>L. Kahn, N. S. Almeida, and D. L. Mills, *Phys. Rev. B* **37**, 8072 (1988).
- <sup>6</sup>D. N. Christodoulides and R. I. Joseph, *Opt. Lett.* **13**, 794 (1988).
- <sup>7</sup>P. W. Anderson, *Phys. Rev.* **109**, 1492 (1958).
- <sup>8</sup>N. F. Mott and W. D. Twose, *Adv. Phys.* **10**, 107 (1961); I. Ja. Goldsheid, S. A. Molchanov, and L. A. Pastur, *Funct. Anal. Appl.* **11**, 1 (1977); H. Kunz and B. Souillard, *Commun. Math. Phys.* **78**, 201 (1980).
- <sup>9</sup>D. L. Shepelyansky, *Phys. Rev. Lett.* **70**, 1787 (1993).
- <sup>10</sup>M. I. Molina and G. P. Tsironis, *Physica D* **65**, 267 (1993), and references therein.
- <sup>11</sup>L. J. Bernstein, K. W. DeLong, and N. Finlayson, *Phys. Lett. A* **181**, 135 (1993).
- <sup>12</sup>S. Dutta Gupta and D. S. Ray, *Phys. Rev. B* **38**, 3628 (1988); **40**, 10 604 (1989); **41**, 8047 (1990).
- <sup>13</sup>L. M. Kahn, K. Huang, and D. L. Mills, *Phys. Rev. B* **39**, 12 449 (1989).
- <sup>14</sup>St. Pnevmatikos, O. Yanovitskii, Th. Fraggis, and E. N. Economou, *Phys. Rev. Lett.* **68**, 2370 (1992); E. N. Economou, O. Yanovitskii, and Th. Fraggis, *Phys. Rev. B* **47**, 740 (1993).
- <sup>15</sup>K. Schmidt and M. Springborg, *Synth. Met.* **55-57**, 4473 (1993); *J. Phys. Condens. Matter* **5**, 6925 (1993).
- <sup>16</sup>M. Johansson and R. Riklund, *Phys. Rev. B* **49**, 6587 (1994); B. Lindquist, M. Johansson, and R. Riklund, *ibid.* **50**, 9860 (1994).
- <sup>17</sup>D. Hennig, G. P. Tsironis, M. I. Molina, and H. Gabriel, *Phys. Lett. A* **190**, 259 (1994); N. Sun, D. Hennig, M. I. Molina, and G. P. Tsironis, *J. Phys. Condens. Matter* **6**, 7741 (1994).
- <sup>18</sup>H. Hiramoto and S. Abe, *J. Phys. Soc. Jpn.* **57**, 1365 (1988).
- <sup>19</sup>T. Geisel, R. Ketzmerick, and G. Petschel, *Phys. Rev. Lett.* **66**, 1651 (1991); in *Quantum Chaos—Quantum Measurement*, edited by P. Cvitanović, I. Percival, and A. Wirzba (Kluwer Academic, Dordrecht, 1992), p. 43.
- <sup>20</sup>H. Hiramoto and S. Abe, *J. Phys. Soc. Jpn.* **57**, 230 (1988).
- <sup>21</sup>M. Dulea, M. Johansson, and R. Riklund, *Phys. Rev. B* **45**, 105 (1992).
- <sup>22</sup>D. E. Katsanos, S. N. Evangelou, and S. J. Xiong, *Phys. Rev. B* **51**, 895 (1995).
- <sup>23</sup>S. Aubry and G. André, *Ann. Isr. Phys. Soc.* **3**, 133 (1980); J. Avron and B. Simon, *Duke Math. J.* **50**, 369 (1983); C. Tang and M. Kohmoto, *Phys. Rev. B* **34**, 2041 (1986); Y. Last, *Commun. Math. Phys.* **164**, 421 (1994).
- <sup>24</sup>I. Guarneri, *Europhys. Lett.* **10**, 95 (1989).
- <sup>25</sup>H. Hiramoto and M. Kohmoto, *Int. J. Mod. Phys. B* **6**, 281 (1992), and references therein.
- <sup>26</sup>J. F. Weisz, M. Johansson, and R. Riklund, *Phys. Rev. B* **41**, 6032 (1990).
- <sup>27</sup>M. Kohmoto, L. P. Kadanoff, and C. Tang, *Phys. Rev. Lett.* **50**, 1870 (1983); S. Ostlund, R. Pandit, D. Rand, H. J. Schellnhuber, and E. D. Siggia, *ibid.* **50**, 1873 (1983); A. Sütö, *Commun. Math. Phys.* **111**, 409 (1987); *J. Stat. Phys.* **56**, 525 (1989); J. Bellissard, B. Iochum, E. Scoppola, and D. Testard, *Commun. Math. Phys.* **125**, 527 (1989).
- <sup>28</sup>A. Bovier and J.-M. Ghez, *Commun. Math. Phys.* **158**, 45 (1993); **166**, 431 (1994).
- <sup>29</sup>J. Bellissard, in *Number Theory and Physics*, edited by J. M. Luck, P. Moussa, and M. Waldschmidt, Springer Proceedings in Physics Vol. 47 (Springer-Verlag, Berlin, 1990), p. 140; J. Bellissard, A. Bovier, and J.-M. Ghez, *Commun. Math. Phys.* **135**, 379 (1991).
- <sup>30</sup>M. Queffelec, *Substitution Dynamical Systems—Spectral Analysis*, Lecture Notes in Mathematics Vol. 1294 (Springer, Berlin, 1987).
- <sup>31</sup>M. Dulea, M. Johansson, and R. Riklund, *Phys. Rev. B* **46**, 3296 (1992); **47**, 8547 (1993).